- ELECTRONIC SUPPLEMENTARY INFORMATION -

Amplifying Vibrational Circular Dichroism by Manipulation of the Electronic Manifold

Sérgio R. Domingos, Matthijs R. Panman, Bert H. Bakker, Wybren Jan Buma, and Sander Woutersen
Van 't Hoff Institute for Molecular Sciences, University of Amsterdam, Science Park 904, 1089 XH, The Netherlands

Frantisek Hartl
Department of Chemistry, University of Reading, Whiteknights, Reading RG6 6AD, United Kingdom

Contents

I. Experimental Methods 1
A. Synthesis and characterization of **1** 1
B. VCD-Spectroelectrochemical Instrumentation 1
C. Cyclic Voltammetry 2
D. UV-Vis spectra (voltage dependent) 2
E. Quantum-chemical Calculations 2
1. Absolute Configuration and Conformation 2
2. Excitation Energies and Magnetic Transition-Dipole Moments 4
3. Difference Density Plots 4

References 4

I. EXPERIMENTAL METHODS

A. Synthesis and characterization of 1

A mixture of 2.50 g of 1,8-naphthalic anhydride and 2.0 g of L-alanine methyl ester Hydrochloride (Aldrich) and 4 ml of TEA in 150 ml of methanol under Ar was refluxed for 15 h. After approximately 1 hour of reflux a clear solution was obtained. The brown solution was concentrated with a rotavap to give a pale brown solid residue. Standing at room temperature a precipitate is formed. After cooling in ice the precipitate was filtered off, washed with cold methanol and dried in vacuum. Yield: 1.772 g, mp.156-8° C (needles). The procedure was repeated with D-alanine methyl ester hydrochloride (Aldrich). The optical rotation of (R)-1 and (S)-1 was measured using the Sodium D line: $[\alpha]_D{}^{20}$=0.131° (concentration: 2.7mg/mL, CH_3CN) and $[\alpha]_D{}^{20}$=−0.123° (concentration 2.6mg/mL, CH_3CN), respectively. For the spectroelectrochemical measurements, tetrabutylammonium hexafluorophosphate (TBAH, Sigma Aldrich) was used as supporting electrolyte. Dry deuterated acetonitrile (CD_3CN) was used as the standard solvent in all the experiments. All samples were prepared under a N_2 atmosphere. Fourier-transform infrared (FTIR) and VCD spectra were recorded on a Bruker Vertex 70 FTIR spectrometer in combination with a PMA 50 module (with 2 cm^{-1} and 4 cm^{-1} spectral resolution, respectively). UV-Vis absorption spectra were obtained with a HP 8453 UV-Vis Spectrophotometer. Conventional cyclic voltammetry (CV) and thin-layer cyclic voltammetry (TL-CV) experiments were carried out with a PA4 potentiostat (EKOM, Poln, Czech Republic) at v=100mVs^{-1} and v=2mVs^{-1}, respectively, allowing controlled-potential electrochemical conversions for qualitative spectroscopic analysis. Infrared spectroelectrochemical (SEC) data were obtained using an IR OTTLE[1] cell for samples of 3.5x10^{-2}M (−)-**1** (10^{-1}M TBAH). VCD-SEC data were obtained using a customized OTTLE cell (see next section) using 7x10^{-3}M (5x10^{-2}M TBAH). Our experiments show that TBAH does not influence the spectra as was previously concluded as well in spectro-electrochemical studies on naphthalimide functionalities closely related to our system[2].

B. VCD-Spectroelectrochemical Instrumentation

In order to combine TL-CV and SEC measurements[3], some practical challenges need to be addressed. We found that TL-CV at high concentrations (>10mM) leads to complications such as formation of aggregates and irreversible chemical processes. To obtain sufficient optical density without the need of highly concentrated samples, we therefore constructed an electrochemical IR cell with a relatively long pathlength (1.2 mm). We customized the IR optically transparent thin-layer electrochemical (OTTLE) cell previously designed and reported on by Krejcik et al.,[1] see Fig. S1. The primary modification involved the polyethylene electrode (PE) spacer into which the three electrodes (working, counter and pseudo-reference) are melt-sealed. A small cut was made in the center of a 5×6 mm Pt mini-grid, and the cut wires were folded outwards, resulting in a cylindric protrusion in the center of the working electrode (Fig. S1) and introducing a 3.5 mm hole in the center of the Pt mini-grid. A 1 mm thick PTFE spacer with a circular aperture of 4 mm sits on top of this construction. This spacer has three major functions: (1) it allows the cylinder to maintain its shape when the CaF_2 window is placed on top; (2) it preserves the thin-layer geometry; and (3) it allows for a large volume of solution only at the probing site so as to increasing the optical pathlength. The 1.2 mm optical pathlength ensures sufficient infrared absorption intensity to measure VCD signals on solutions with concentrations as low as 7×10^{-3} M. The extruded cylindrical shape of the modified mini-grid electrode ensures complete, although relatively slow (3-5 min), electrochemical conversion along the 1.2 mm optical path.

In a regular VCD spectrometer, the resulting small aperture of the spacer would cause significant clipping of the

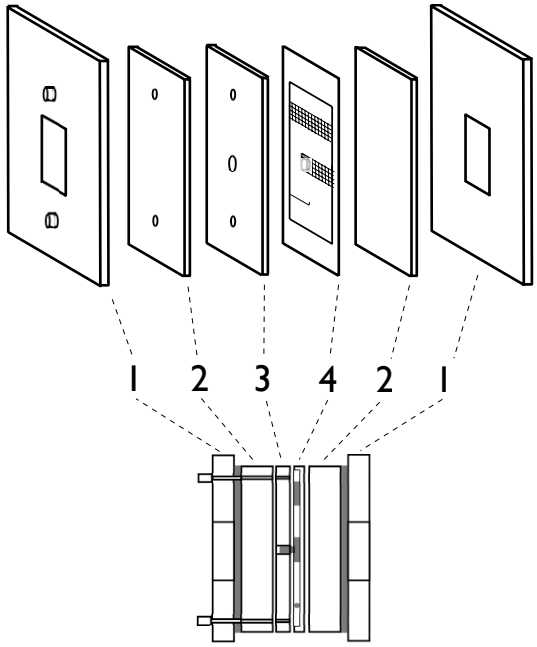

Fig. S1: Schematic drawing of the customized OTTLE cell for VCD measurements: 1. metal holder; 2. CaF_2 window; 3. PTFE spacer (1 mm thick) with a circular aperture (4 mm diameter); 4. custom polyethylene-electrode spacer; from top to bottom: counter electrode; working electrode with cylindrical protrusion in the center; pseudo-reference electrode.

circularly-polarized IR light. An optical telescope was assembled in the PMA 50 sample compartment using two ZnSe lenses of 50 and 38 mm focal lengths. The telescope allows focusing of the circularly-polarized IR beam into the small volume of solution where the electrochemical conversion occurs. The 3 mm beam waist is sufficiently small for all the IR light to be transmitted through the 4 mm diameter hole in the grid of the electrochemical cell. We tested the new construction (cell+telescope) extensively, reproducing quantitatively literature VCD spectra of (R)-(+)-1,1'-Bi(2-naphthol) and (S)-(−)-1,1'-Bi(2-naphthol).[4] To determine the VCD baseline two approaches have been employed. In the first VCD spectra of the two enantiomers are subtracted and the resulting spectrum is divided by two. In the second the spectrum of the pure solvent is subtracted from the VCD spectrum of the sample. We found that both methods lead to the same result.

C. Cyclic Voltammetry

Fig. S2 depicts the cyclic voltammogram of (−)-**1**.

D. UV-Vis spectra (voltage dependent)

Fig. S3 shows the voltage-dependent UV-Vis spectral changes of (S)-**1** in CD_3CN. We can clearly observe the appearence and increase of four bands at lower energies in the radical anion when compared with the neutral species.

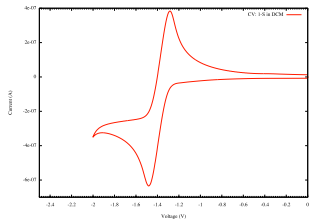

Fig. S2: Cyclic voltammogram of (−)-**1** vs Fc/Fc^+ in CD_3CN with TBAH as supporting electrolyte.

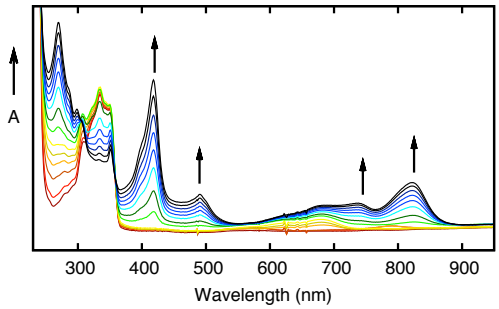

Fig. S3: Voltage-dependent UV-Vis spectra within voltage range (−1.2,−1.39) V.

E. Quantum-chemical Calculations

1. *Absolute Configuration and Conformation*

In the previous part we have shown that modulation of the electronic excitation energies can be used advantageously to enhance VCD signals. Here, we will be concerned with the absolute configuration and conformation of the compounds used in the present study. To this purpose four different conformers were identified at the AM1 semi-empirical level for both the neutral and the anionic species. The geometries of these conformations served as a starting point for further optimization at the DFT level of theory using the B3LYP functional and the 6-31G(d) and 6-31+G(d,p) basis sets for neutral and radical anion species, respectively. All calculations were performed with Gaussian 03[5]. The final structures that were thus obtained for the neutral molecule are displayed in Figure S4. For the radical anion the same conformations were obtained with only minor changes in geometrical parameters.

Conformers **1a** and **1b** were found to have the lowest energy in both the neutral and anionic forms. For the neutral conformer, **1b** has the lowest energy with conformer **1a** being 0.7 kcal/mol higher in energy, for the anion the energies of the two conformers are within 0.01 kcal/mol. Such energy differ-

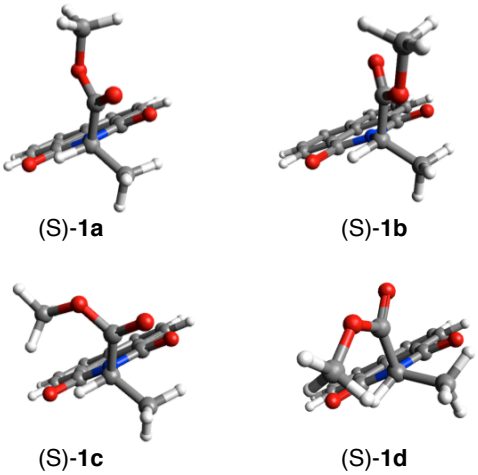

Fig. S4: Equilibrium geometries obtained at the B3LYP/6-31G(d) DFT level of theory, for the four conformations of (S)-**1**, ordered from lower to higher energy **a–d**.

ences are far smaller than the accuracy of the calculation. We therefore have to assume that both conformers can in principle contribute to the observed IR and VCD spectra. Neutral (anionic) conformers **1c** and **1d**, on the other hand, have energies that are 13.9 (13.0) and 10.4 (10.5) kcal/mol higher than the lowest energy conformer, and can thus safely be ruled out as being present under the employed experimental conditions.

At each of the optimized geometries harmonic force fields were calculated. From the calculated dipole and rotational strengths IR and VCD spectra were simulated assuming Lorentzian band shape with a width of 2 and 4 cm^{-1}, respectively, and scaling the computed frequencies with a factor of 0.97. In Fig. S5 we show the observed and calculated IR and VCD spectra for the neutral species of (S)-**1**. In general, good agreement is observed between the experimental spectra and the predicted spectra of conformations that are expected to be dominantly present. From comparison of the observed spectra in Fig. S5 and calculated spectra for the (S) configuration, we assign the absolute configuration as (−)-(S)-**1**.

For example, the sign pattern and intensities predicted for the VCD spectra of conformers **1c** and **1d** are irreconcilable with the experimentally observed patterns, confirming their absence under employed experimental conditions. A more detailed comparison of the spectra predicted for conformers **1a** and **1b** with the experimental spectra rapidly leads to the conclusion that the IR spectrum is not sensitive enough to distinguish the subtle geometrical differences between **1a** and **1b**, and therefore cannot provide a means to access their configuration to the experimental spectrum. The VCD spectrum has in that respect much more resolving power. Inspection of the 1400–1800 cm^{-1} region shows that the experimental spectrum — and in particular the sign pattern — is in significantly better agreement with the predicted spectrum of conformer **1a** than of **1b**. Nevertheless, the oppositely predicted sign of the

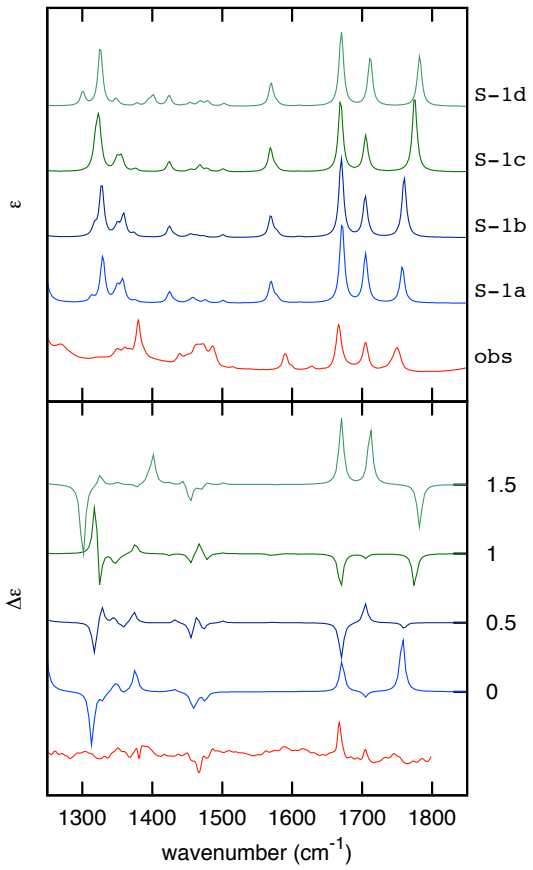

Fig. S5: Observed and calculated IR (upper-panel) and VCD (lower-panel) spectra for the neutral species of (−)-(S)-**1**. All spectra are scaled and normalized for clear comparison.

band at 1700 cm^{-1} and the intensity of the 1750 cm^{-1} band remains at odds with the observed spectrum.

Recently, the concept of robust normal modes has been introduced.[6] Such modes have been defined as modes for which the angles between the electronic and magnetic transition dipole moments differ by at least 30° from 90° and have rotational strengths of significant magnitude. In that study it was concluded that preferably only robust modes should be employed for configurational and conformational assignments as other modes are too sensitive to the finer details of the calculations. Analysis of the modes of (S)-**1** in the 1400-1800 cm^{-1} region shows that in the present case none of the modes can be marked as robust. In fact, we find for the modes at 1700 cm^{-1} and 1750 cm^{-1} angles that are close to 90°, rationalizing the discrepancies between experiment and theory observed for these two modes.

In Fig. S6 we show the observed and calculated IR and VCD spectra for the radical anion species of (−)-(S)-**1**. Again, we find very good agreement between experimental and calculated IR spectra, but no distinct markers that would enable us to rule out one or more conformers. However, as was argued for the neutral species, the absence of spectral signatures

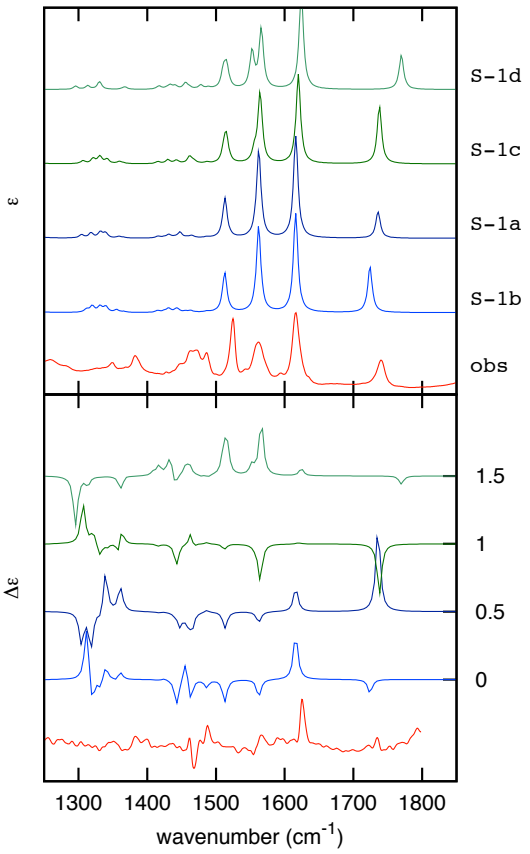

Fig. S6: Observed and calculated IR (upper-panel) and VCD (lower-panel) spectra for the anion species of (−)-(S)-**1**. All spectra are scaled and normalized for clear comparison.

of **1c** and **1d** in the VCD spectrum of the radical anion indicates that these conformers are not present. It is considerably more difficult to determine in which ratio conformers **1a** and **1b** are present. Comparison of the experimental VCD spectrum with the predicted spectra for **1a** and **1b** in the spectral region where the experimental spectrum has relevant intensity shows a fair agreement, but the only mode that appears to be truly distinctive is the one at 1750 cm^{-1}. We recall that the two conformers are predicted to have similar energies. Indeed, analysis of the experimental spectrum in terms of varying contributions of the predicted spectra for **1a** and **1b** indicates that it is rather plausible that both conformers contribute to the experimental spectrum.

2. *Excitation Energies and Magnetic Transition-Dipole Moments*

Table SI lists the excitation energies for the first ten electronic excited states of the radical anion of (S)-**1** and the magnitude of the magnetic transition dipole moment associated with each of the electronic states.

Table SI: Ground to excited state magnetic transition magnetic dipole moments (atomic units) and excitation energies for the first 10 electronically excited states of the radical anion of (S)-**1**.

State	$\lvert\mu_{mag}\rvert$	Excitation Energy (eV)
1	0.07185	1.8272
2	1.61079	1.9221
3	0.00684	2.6033
4	0.10306	2.7643
5	0.17983	3.2404
6	0.05857	3.4285
7	0.08959	3.5600
8	0.35100	3.6869
9	0.50402	3.6964
10	0.08378	3.8510

3. *Difference Density Plots*

Difference density plots (isovalue 0.004) for the first (left) and second(right) excited states ($D_1 - D_0$) and ($D_2 - D_0$), respectively, from a TD-DFT (B3LYP/6-31G(d,p)) calculation on the radical anion of (S)-**1**, where blue color represents negative (lost ground-state) density and the red color positive (gained excited-state) density.

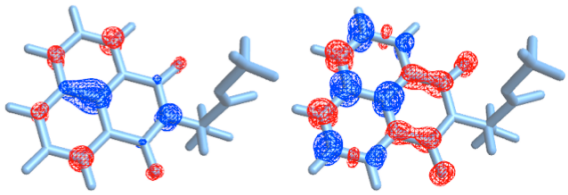

Fig. S7: Difference density plots for D_1 and D_2

[1] M. Krejcik, M. Danek, and F. Hartl, J. Electroanal. Chem. **317**, 179 (1991).
[2] D. Jagesar, F. Hartl, W. Buma, and A. Brouwer, Chem. Eur. J. **14**, 1935 (2008).
[3] W. Kaim and J. Fiedler, Chem. Soc. Rev. **38**, 3373 (2009).
[4] V. Setnicka, M. Urbanova, P. Bour, V. Kral, and K. Volka, J. Phys. Chem. A **105**, 8931 (2001).
[5] M. J. Frisch, G. W. Trucks, H. B. Schlegel, G. E. Scuseria, M. A. Robb, J. R. Cheeseman, J. A. Montgomery, Jr., T. Vreven, K. N. Kudin, J. C. Burant, et al., *Gaussian 03, Revision C.02* (2004), Gaussian, Inc., Wallingford, CT.
[6] V. P. Nicu and E. J. Baerends, Phys. Chem. Chem. Phys. **11**, 6107 (2009).